Quality control of safety belts by machine vision inspection for real-time production

Daniel Ponsa, Robert Benavente, Felipe Lumbreras,

Judit Martínez and Xavier Roca

Computer Vision Center and Dept. Informatica (UAB)

Edifici O, Campus UAB,

08193 Bellaterra (Barcelona), Catalonia. Spain

phone: +34 93 581 18 28

fax: +34 93 581 16 70

e-mail : {daniel|robert|felipe|judit|xavir@cvc.uab.es

18th June 2002

Abstract

Safety belts are specific fabrics manufactured ensuring the highest performance. Their manufacturing process not only has to assure its endurance to high tensions strength, but also has to guarantee its correct visual appearance. Safety belts must not contain fibre breaks, knots, thickness variations, etc. Such defects imply the non-fulfillment of rigorous safety standards.

This paper describes the development of a computer vision inspection system, which control safety belts at a speed rate of 2 m/s. This inspection rate has been achieved by means of a parallel architecture and the use of optimized vision algorihms

Keywords: machine vision, quality control, woven inspection, texture.

1 Introduction

Belts are made in a normal textile process where wrap and weft are woven. The belt structure changes radically from customer to customer because each one has its own models (see figure 1). A very demanding objective in safety belt manufacturing is an error–free final production due to quality are not only related to visual appearance but also to mechanical properties strongly related to safety.We have categorized defects according to its visual appearance and location, some examples are shown in figure 2. These defects share similarities with those of the textile industry [1] with some special features and cases specific of this fabric. To achieve the error–free goal, quality control of the production has to be extremely reliable. Currently, this task is mostly carried out by laser inspection systems. These systems examine the belt while it passes through a set of laser diodes (at a speed up to 2 m/s). When inspection system detects one defect, the traction system that moves the belt is stopped and a human operator will repair the error if it is possible, otherwise they will mark and the section of the belt containing it will be cut afterwards. Those systems can only detect defects that jut out of the belt profile, without taking into account any plane texture error. Another important drawback is that these systems are not able to quantify precisely the size of the detected defects, making difficult to establish a good acceptance/rejection criterion. Moreover, when there is an extraordinary rate of false reject defect, the systems constantly stop the motor and all the intermediate continuous belt buffers in the manufacturing process fill.

Therefore, the key aspects that an automatic inspection system should incorporate are: (i) to detect the whole set of possible defects that can be done in the production, (ii) to give a useful information to the human operators (as for example where the defect is placed or statistics about the production), (iii) to be flexible to inspect new type of belts, and finally, (iv) to be easy to set the right set of inspection parameters, minimizing the number of false accepts and rejects, these points are the base of the new system machine vision developed.

In section 2 we explain the different parts of the system and the hardware solutions adopted. Section 3 explains the algorithms proposed to solve the inspection problem. Section 4 is a brief summary of the results and in the last section we sum up to some conclusions about our proposed system

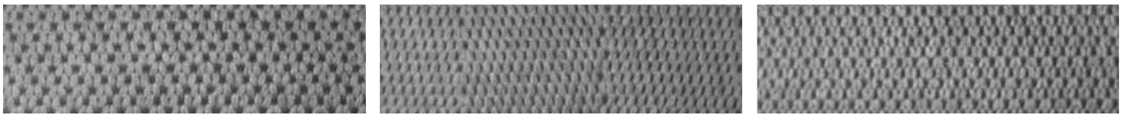

Figure 1: Three different types of belts

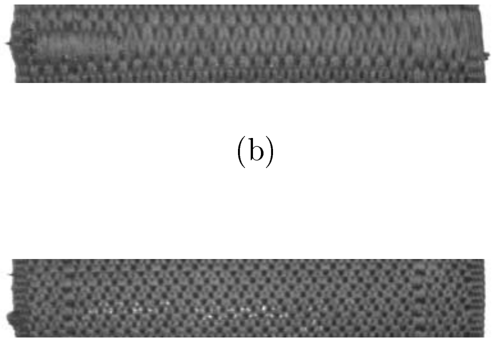

(a) (b) (c) (d)

Figure 2: (a) irregular contour (edge defect), (b) weft not woven (texture break), (c) fraying edge, (d) knot and stains.

2 Image Acquisition System

Due to the high speed requirements of the system, a parallel architecture has been adopted. The image acquisition system is composed by a total of four B/W progressive Jai M-30 cameras, two for each belt side. Each one of the cameras is connected to a slave computer, see figure 3, where the images are processed by a Matrox MeteorII/MC board. When one of the four slaves detects a defect, it is reported to the master computer which compiles the partial results, synchronizes the errors (the same error can be detected by different slaves) and stops the production line when the error reaches the stopping point.

The four slaves and the master are standard PCs with an Intel Pentium III processor running under the Windows NT operative system.

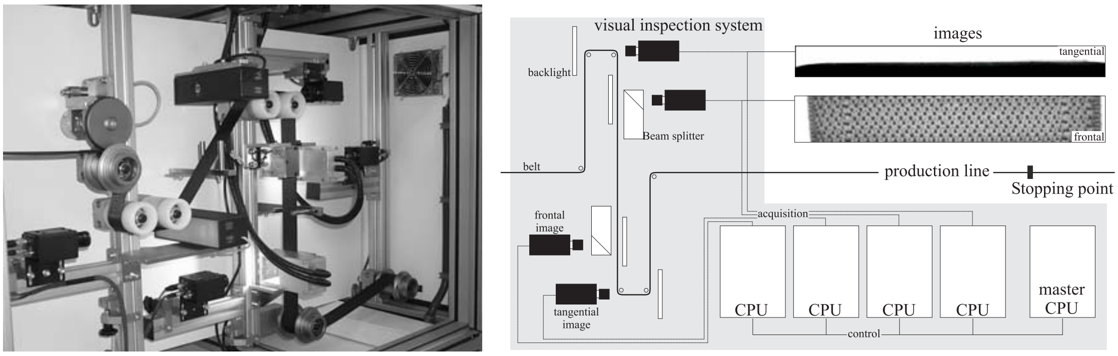

Figure 3: Scheme of the visual inspection system

In order to be able to detect all the different kinds of flaws that may appear on the woven belts, two different views of each side of the belt are acquired. For each side, one of the cameras takes a frontal image of the belt surface while the other provides a tangential view.

The frontal image allows the detection of all the flaws that do not jut out over the surface of the belt, such as knots, missing threads, stains and, in general, any kind of texture pattern failure. The frontal images are also used to study the uniformity of the belt edges. Thus, defects that only appear on the belt edges, such as loose threads and variation on the width of the belt, can also be detected.

The purpose of the tangential image is the detection of loose threads on the surface of the belt, which are not visible in the frontal view.

An overview of the acquisition system used and an example of each kind of image (frontal and tangential) can be seen in figure 3.

2.1 Illumination system

Both frontal and tangential images are acquired under diffuse backlight illumination in order to obtain high contrast images. Hence, the region of the image corresponding to the belt can be easily segmented from the background.

Since the aim of the tangential subsystem is only the detection of loose threads over the belt surface, the backlight illumination is enough for tangential images.

However, in the frontal images, we need a high resolution view of the texture pattern of the belt. This implies the use of direct light over the surface of the belt. Therefore, the frontal subsystem also includes a diffuse frontal coaxial illumination (beam splitter) in order to avoid spatial light variations and providing a constant light over all the surface of the belt.

2.2 Image acquisition speed

All the cameras are configured in partial scan mode in order to obtain "narrow" images. The election of the image sizes was conditioned by two factors. On the one hand, there is a precision requirement on the localization of the flaw. After a defect is detected, the production line should be exactly stopped when the defect reaches the stopping point. The accuracy required for this stop is ± 2 cm for the proposed system. This means that the images should not include more than 2 cm of belt in order to fulfil the precision requirement. Thus, the frontal image is 768×110 pixels which correspond to a length of 1.6 cm of belt. For the tangential images, a size of 768×66 pixels was chosen. In this case, the portion of belt seen on the images depends on the fitting up of the production line in front of the camera.

On the other hand, partial scan mode allows acquiring up to 360 frames per second. As it was mentioned before, the maximum traction speed of the line is 2 m/s This means that, for the frontal cameras, we should process at least 125 images per second in order to inspect all the belt surface. This implies that each image has to be processed in 8 ms.

3 Defect Segmentation Algorithm

In this section we present a set of optimized algorithms [2] adapted to each part of the inspected belt that allows us to get a maximum performance of the whole system.

The implemented algorithms are very basic and can be found in fundamental books of computer vision [3, 4] and machine vision [5, 6].

3.1 Tangential

Tangential cameras give information mainly of bad woven, frayed threads and bulky zones. These defects jut out the profile shown in the tangential views of the belt, and have to be detected and also quantified to overcome the facilities of existing laser inspection systems. This task can be done almost directly if the traction system of the production line assures an stable position of the belt profile along time. In that way, the inspection process reduces to detect and analyse the belt pixels over a given image coordinates. However, having a fixed position for the

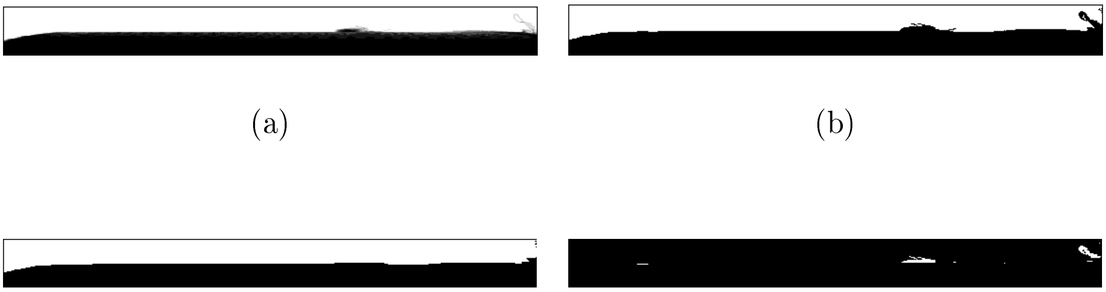

(a) (b)

(c) (d)

Figure 4: Sequence of the tangential process: (a) initial image, (b) threshold, (c) morphological filtering, and (d) difference between threshold image and the filtered image.

belt profile requires the use of stabilizing components in the traction system, that prevent from obtaining high-contrast images of the belt. For this reason, a method that presents independence of the position of the belt profile has been developed. The method requires the belt profile to remain approximately parallel to the image frame, a condition assured by the traction system. Given an image, its pixels are firstly classified into belt or background pixels. Secondly, a morphological opening (equation 1) [7] is applied to belt pixels to obtain the *correct* profile as result of this operation (see figure 4(c)), note that it doesn't have to correspond exactly to an straight line.

$$X_B = (X \ominus \breve{B}) \oplus \breve{B}. \tag{1}$$

where $\breve{B}$ is the following structuring element (11111)

Finally, this correct profile is used to detect and to characterize defects. Figure 4 summarizes how the overall procedure is implemented in practice.

The initial classification of the image pixels is done by means of an adaptative binarization algorithm. The image is first subdivided into small regions, where the backlight illumination can be assumed as homogeneous. Then, the upper zone of each region (which corresponds to the backlight illumination) is analyzed, and a classification threshold is determined. Regions are then binarized, and the resulting image is then compacted to 1 *bit/pixel* to perform the remainder process at a maximum speed rate. The opening operation using $\breve{B}$ is applied, and the resulting image is XOR–operated with the original binary one, obtaining a resulting image where defects are represented as blobs. Analyzing these blobs, defects are localized and characterized, enabling to establish different acceptance/rejection criteria depending on size, shape or localization.

3.2 Frontal

Frontal cameras are used to detect defects due to a bad weave process of the belts, and to check regularity of contours. These errors are detected by processing different regions of the belt image with an *ad-hoc* algorithm that focus on the specific errors that the concrete region may suffer.

In all belt designs it is possible to distinguish three different regions, we will call them: *Contour*, *1D Texture* and *2D Texture* (see figure 5), and each one has associated a specific algorithm.

These regions are placed, for each new belt, at a learning stage, depending on its design structure. These regions of interest are dynamically placed in each acquired image in order to be independent the imprecise positioning of the belt. Following subsections will describe the processing algorithms applied to each region.

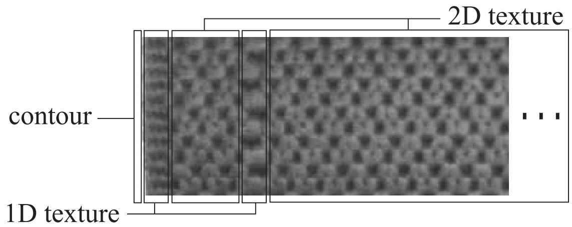

Figure 5: The three regions for frontal images where the inspection is done. Each region has its specific algorithms.

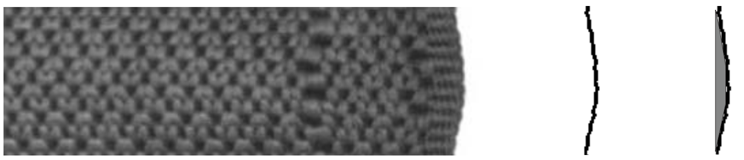

(a) (b) (c)

Figure 6: (a) irregular contour, (b) edge detection (binarized), and (c) difference between ideal and real straight line.

3.2.1 Contour defects

In the contour regions we try to detect frayed threads, knots and inhomogeneities of the contour. To detect these defects we first determine the lines that join the upper and the lower extremes of each belt side and we measure the error between the ideal and real straight line (which is calculate a using finite differences in the x direction). It gives us an objective criterion to detect this kind of errors (see figure 6).

3.2.2 1D-Texture

We will call 1D textures to those regions of the belt that can be analyzed as an unidimensional signal. These textures are usually found along the borders of the belt and occasionally as an inside region, depending on the belt design (see figure 5).

Defects occurring in the 1D texture regions are detected as a change in periodicity of the unidimensional signal. Since the periodicity of a signal is more easily analyzed in the Fourier domain, we will apply the Fourier Transform to the unidimensional signal and search for variations in this domain. In particular, defects will be detected as variations of the dominant frequency in comparison to the learned parameters in the definition stage.

To process these regions, represented by the image $\mathbf{I}$, we first transforms it into a unidimensional signal making the horizontal projection by accumulating the pixel values of the texture into a column vector $\mathbf{v}$, computed as:

$$\mathbf{v}(i) = \sum_j \mathbf{I}(i,j). \tag{2}$$

The aspect of these vectors are shown in figure 7 (a) and (b).

Before to apply the Fast Fourier Transform (FFT) to $\mathbf{v}$ and in order to reduce influences of the rectangular windowing of the unidimensional signal, we will first multiply this signal by a Hamming function $\mathbf{h}$ [8], equation 4. Therefore, we compute:

$$\mathbf{f_h}(k) = \frac{1}{N} \sum_{i=1}^{N} \mathbf{v_h}(i)\, e^{\frac{j2\pi}{N} ik}, \tag{3}$$

for $k = 0, ..., N-1$, being N the number of rows in $\mathbf{I}$, and

$$\mathbf{v_h}(i) = \mathbf{v}(i) \cdot (0.54 - 0.46 \cos(\frac{2\pi i}{N-1})). \tag{4}$$

The dominant frequency is selected as the value of $k \neq 0$ where $\mathbf{f_h}$ takes its maximum

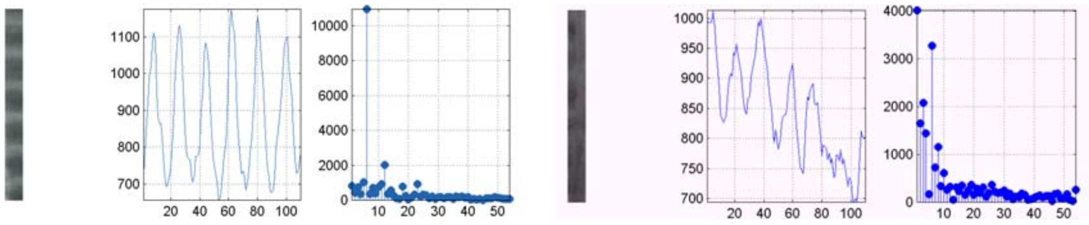

(a) (b)

Figure 7: On the left of each figure we can see the 1D texture region, image **I**, in the middle the unidimensional signal by horizontal accumulation, vector **v**, and on the right the frequency spectra. (a) Correct Texture 1D , (b) Defective Texture 1D

value. Variations of this feature from the expected one allow us to detect defects in 1D textures (see figure 7).

3.2.3 2D-Texture

Frontal images are mainly formed by a bidimensional texture that gives to the belt its appearance (see figure 1). Some of the defects detected from other viewpoints such as tangential images also appear, but there are a new set of defects that can only be seen in these images because they do not have any effect on the belt thickness. All the errors on 2D texture regions have the same features, that is, they break the periodicity of the bidimensional texture defined by the fabric. To detect them, as in the section 3.2.2, we take profit of the fact that analysed region presents a repetitive pattern.

The study of the lack of repetitiveness in this bidimensional texture regions make us to confront an important problem. The high speed of the production line requires that a very low processing time is assigned to the vision inspection system; otherwise, our inspection process would become a bottleneck. As we have said before, we have 125 images per second of 768×110 pixels, therefore we have 8 ms to process the image and deliver the result about its quality. This restriction on processing time can be alleviate using several cameras acquiring different parts of the belt at the same time. In that way, the increase of time obtained with a reasonable number of cameras will not be enough to use general techniques for texture analysis based on spectral methods as Gabor filters or wavelets transform [9, 10]. Rejecting spectral methods, a first attempt can be learning in an initial stage a pattern of the whole and correct texture in order to compare later with the acquired images. But, due to the fact that these new images are not acquired at the same position (horizontally, the belt can be moved along the spindle, and vertically, the acquisition is not synchronized to the period of the texture), then, we need to register the two images, the learned pattern and the image to be analyzed, and this is a high time–consuming task. Previous considerations gave us the conclusion that we needed a fast solution that can be adapted to slight position changes in the images as it occurs in our problem.

The solution we have adopted is based on taking the same image that must be analyzed as a pattern for such analysis, that is, the acquired image is the model to itself. We take profit of this repetitiveness comparing several parts of the same image avoiding changes in position. Firstly, in a previous learning stage, each bidimensional texture of a belt is characterized by a displacement vector $\mathbf{d}=(d_x, d_y)$. Components d_x and d_y of this vector are the length of the repetitiveness period in each direction, that is, any part of the image displaced by this vector is taken to a similar image

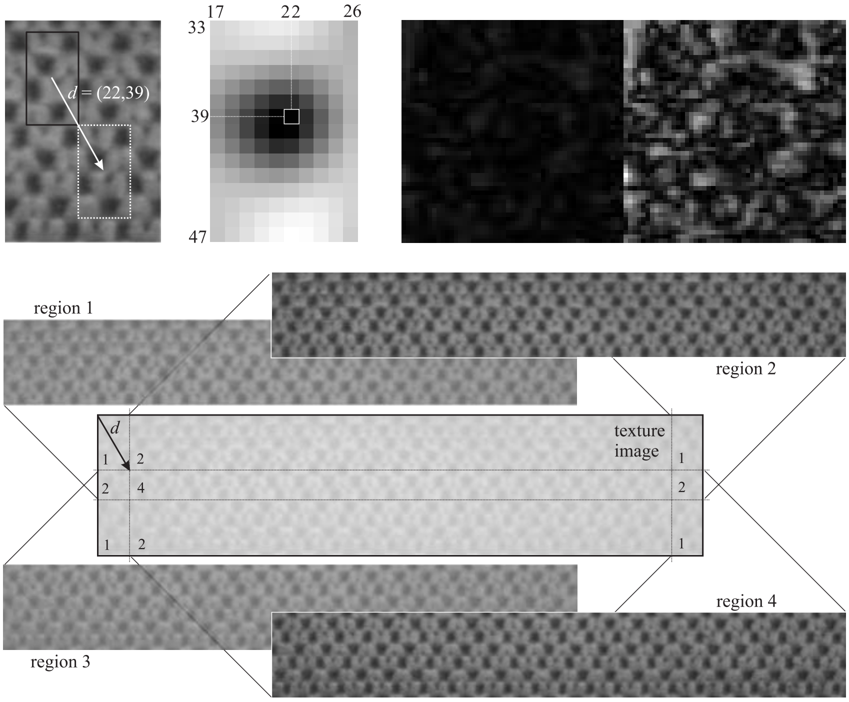

Figure 8: Top: displacement vector pointing to similar regions; minimum difference for different vectors used to calculate d; remainder for and area without defects of 50×50 pixels and its contrast maximization (values are lower than 20% of the maximum value). Bottom: the four regions used to avoid boundary effects; some parts of the image are evaluated more than once, so we need several weights as show the numbers.

area, see figure 8. In order to avoid boundary effects we split each texture image in four overlapping regions. The model image is built moving each region to the opposite corner in the image and averaging the results because some image areas are computed more than once. The image and the model image are compared by thresholding the absolute value of the difference. Next, we perform fast filtering with morphological opening over the remainder. Then, computing some statistics of the blobs we can detect different kind of defects related to this area.

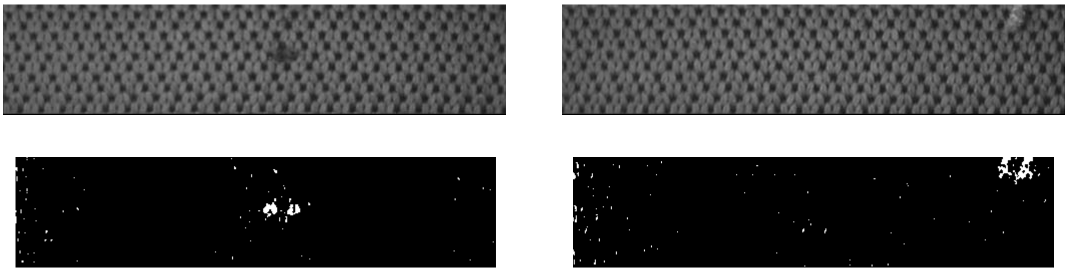

Figure 9: Top, defective textures. Bottom, result of the 2D–texture defect detection algorithm.

Figure 9 shows some results of this part where defects are detected. Defective areas correspond to the bigger white areas in the binary image.

4 Experiments and Results

The improvement achieved by the proposed system has been measured by the execution of different performance tests. These tests consisted of checking the results given by the vision system, versus the laser inspection system in the first test, and the vision system versus a human expert in a second test.

In the first case, the machine vision system was serially appended with the laser system. This test let us show to the final user that the new system can detect more defects without increasing the number of false rejections given by the laser system.

Second test allowed to evaluate the number of false acceptations produced by the system. In this test, more than 17.000 strips were checked, each one being 3 meters long. These strips are the final product given to customers to build the final safety belt mounted on the car. The results showed that the operators found 120 strips with some kind of errors (false acceptations, not detected by the vision system), this means 7.000 parts per million (ppm) (less than 1%) and a reduction of around 50% of false acceptations with respect to the laser machine.

The other test done was to check, by human operators, the product that was ready to be sent to the customers inspected previously by the machine vision system. With this test it was possible to evaluate the false acceptations of the machine. In this test, more than 17.000 strips were cheched, each one being 3 meters long. These strips are the final product given to customers to build the final safety belt to be mounted on the car. The results showed that the operators found 120 strips with some kind of errors (false acceptations, no detected by the vision system), this mean 7.000 parts per million (ppm) (less than 1%) and a reduction of around 50% of false acceptations with respect to the laser system.

Finally, in figure 10 we can see some results detected by the vision system where defects are located.

5 Conclusions

The system we have presented in this paper is able to control the whole belt quality at high speed, overcoming the performance of the previous laser system. This is achieved subdividing the problem into few specific problems that require the process of small images quickly. For each one of these specific problems we have developed fast solutions, achieving the final solution compiling and integrating the different results. We want to give special relevance to the 2D–texture analysis process and its capability to measure the importance of a defect, allowing to establish reliable

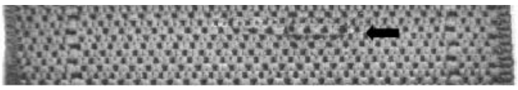

(a)

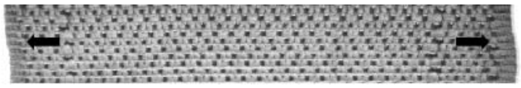

(b)

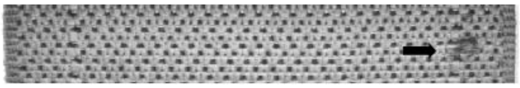

(c)

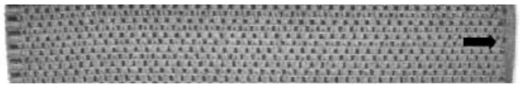

(d)

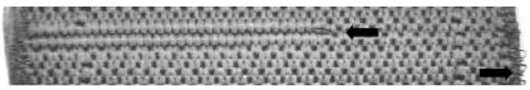

(e)

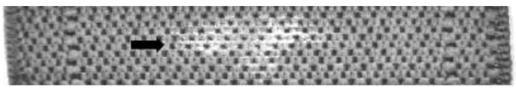

(f)

Figure 10: Defects detected by the system(a) dip (broken texture), (b) irregular contour (edge defect), (c) knot in surface (broken texture), (d) weft not woven to the warp (edge defect), (e) thread lost in the weft (broken texture) and fraying edge (edge defect), (f) stain (broken texture).

acceptance/rejection criterion.

Presently, the rate of inspection is at 2m/s, and this is the current speed of the production line. It means that the visual inspection process is not a bottleneck of the system as it occurred with the laser inspection system. Finally, we want to emphasize that the system uses an standard PC architecture, which means that in the future its performance can be easily improved by a hardware upgrading.

Acknowledgement

This work has been partially funded by projects 95–0510–OP, TIC2000–0382 and UAB FIPD grant.

References

[1] B. Nickolay, K.-H. Schicktanz, and H. Schmalfuß, *Automatic Textil Inspection (Studie für die Textilindustrie).* 1993.

[2] J. E. Lecky, "Using MMX technology to speed up machine vision algorithms (tutorial)."

[3] R. Gonzalez and P. Wintz, *Digital Image Processing.* Addison Wesley Publishing Company, 1992.

[4] B. Jähne and H. Haußecker, *Computer Vision and Applications.* Academic Press, 2000.

[5] M. Burke, *Handbook of machine vision engineering.*, vol. I: Image Acquisition. Chapman & Hall, 1996.

[6] H. R. Myler, *Fundamentals of Machine Vision.* SPIE, 1998.

[7] J. Serra, *Image analysis and mathematical morphology.* Academic Press, 1982.

[8] W. K. Pratt, *Digital Image Processing.* New York: Wiley — Interscience, 1978. General.

[9] J. Escofet, R. Navarro, M. Millan, and P. J.M., "Detection of local defects in textile webs using gabor filters," *Optical Engineering*, vol. 37, no. 8, pp. 2297–2307, 1998.

[10] J. Weickert, "A real-time algorithm for assessing inhomogeneities in fabrics," *Real–Time Imaging*, vol. 5, pp. 15–22, February 1999.